https://doi.org/10.5194/hess-2020-248
Preprint. Discussion started: 21 July 2020

Hydrology and Earth System Sciences
Discussions
Open Access
EGU

Contrasting physical controls on phosphorus transport to shallow groundwater at the hillslope scale

Maelle Fresne[1,2,3], Phil Jordan[2], Per-Erik Mellander[1,3], Karen Daly[3], Owen Fenton[3]

[1]Agricultural Catchments Programme, Teagasc, Johnstown Castle Environment Research Centre, Wexford, Co. Wexford, Ireland

[2]School of Geography and Environmental Sciences, Ulster University, Coleraine, UK

[3]Crops, Environment and Land Use Programme, Teagasc, Johnstown Castle Environment Research Centre, Wexford, Co. Wexford, Ireland

Correspondence to: M. Fresne (Maelle.Fresne@teagasc.ie)

https://doi.org/10.5194/hess-2020-248
Preprint. Discussion started: 21 July 2020

Hydrology and Earth System Sciences
Discussions
Open Access
EGU

Abstract

In well-drained agricultural catchments transport of phosphorus (P) to groundwater (GW) can be controlled by static and dynamic factors and where surface water is GW fed this can lead to elevated P concentrations at the catchment outlet. In order to better control P transport along hillslopes a spatial and temporal conceptual view of P loss to GW must be developed. Initially in the present study, hillslope GW quality and rainfall data were examined for 2017 utilising a transect of piezometers at upslope (US), midslope (MS) and downslope (DS) locations. Two dominant scenarios emerged where GW P concentrations at DS and MS were simultaneously low or at other times DS became elevated and MS remained low. To examine the potential reasons for such scenarios, a one-dimensional hydrological transport model was developed for the unsaturated zone at DS and MS using rainfall and depth specific soil physical and hydraulic data. Results indicated that the DS zone facilitated transport (higher sand content, soil saturated hydraulic conductivity (K_s) and lower soil compaction) with higher modelled concentration peaks towards higher GW P concentrations whereas the MS zone had more potential to attenuate transport (lower soil K_s and higher soil compaction). Moreover, inter-annual variations of GW P concentrations at DS were related to rainfall and GW level. Hence, mitigation strategies should particularly (but not exclusively) focus on reducing P sources in the DS zone. This also indicates a need to identify "hotspots" of facilitated transport to shallow GW using finer scale soil properties surveys. Here, this is defined by low soil compaction, high sand content and soil K_s. However, challenges arise as soil properties can vary in time with soil management and with the difficulty of assessing the transport potential of deeper soil.

1. Introduction

https://doi.org/10.5194/hess-2020-248
Preprint. Discussion started: 21 July 2020


Hydrology and Earth System Sciences
Discussions

Phosphorus (P) is a key nutrient for plant growth and food security (Cordell and White, 2014) but it can also be lost from agricultural land thereby contributing to the eutrophication of surface waters (Withers et al., 2014) which is a continuing global problem (Sinha et al., 2017). Within agricultural catchments, static (e.g. soil, subsoil and geology (Fenton et al., 2017)) and dynamic (e.g. climate (Mellander et al., 2018)) controls on P in groundwater (GW) and surface water are complex. Such controlling factors determine the timing, load, concentration and form of P delivered to a water body (Lintern et al., 2018). Concentrations of P in GW can be influenced by soil properties such as pH and clay % (Mabilde et al., 2017) as well as the presence of macropores or preferential flow paths (Bol et al., 2016; Julich et al., 2017; Fuchs et al., 2010). Bedrock P (sediments) and dissolution of P-rich minerals (McGinley et al., 2016) are also known as internal sources of P in GW. Temporal variations have been related to GW depth (Mabilde et al., 2017) influencing soil redox conditions and P release from Fe-oxides (Neidhardt et al., 2018; Dupas et al., 2015). Hydrological dynamics of hillslopes shallow subsurface flows are highly variable in space and time (Bachmair et al., 2012b) and controlling factors include rainfall (Lehmann et al., 2007; Duan et al., 2017), bedrock topography and permeability (Tromp-van Meerveld and Weiler, 2008; Graham et al., 2010) as well as soil properties (Bachmair and Weiler, 2012a): topography (Bachmair and Weiler, 2012a), infiltration capacity, hydraulic conductivity, drainable porosity, moisture content and vertical and lateral preferential flowpaths (Guo et al., 2019; Anderson et al., 2009). Despite GW P being subject to microbial cycling, subsurface transport, and immobilization (Neidhardt et al., 2018), processes possibly attenuating belowground P, GW contribution to stream P is a concern (Mellander et al., 2016). This can be indicated by a higher contribution of bioavailable P (to total P) associated with a greater proportion of baseflow in rivers (Schilling et al., 2017). Therefore, any interpretation of contrasting P concentrations in GW at different monitoring points within a hillslope must include a variety

https://doi.org/10.5194/hess-2020-248
Preprint. Discussion started: 21 July 2020


Hydrology and Earth System Sciences
Discussions

of these factors. Increased characterisation and knowledge of contrasting scenarios is vital if best management practices on hillslopes are to be implemented correctly (i.e. right measure, right place) to safeguard water quality (Sharpley, 2016). Catchment scale studies with river and GW data, combined with physical data (meteorological and soil data, GW level), have the best opportunity to reveal transport processes from soils to GW and also subsequent delivery to surface water (Melland et al., 2012; Mellander et al., 2016; Mellander et al., 2014).

Combined field and laboratory techniques have used undisturbed (Bacher et al., 2019) or disturbed (Pang et al., 2016) soil, subsoil and bedrock that develop datasets to run model scenarios that best explain the transport of P to GW (Schoumans and Groenendijk, 2000; Schoumans et al., 2009). Different levels of data complexity (from simple to complex) affect transport model outcomes and it is therefore preferable where possible to collect undisturbed soil cores and develop soil physical and hydraulic parameters (Bünemann et al., 2018). Soil physical data such as porosity, saturated hydraulic conductivity (K_s) or bulk density (ρ_b), in combination with soil texture and water storage, can be used in models to assess water and solute transport dynamics through the unsaturated zone to GW (Fenton et al., 2015; Vero et al., 2014), in combination with site specific meteorological data (Gladnyeva and Saifadeen, 2013; Vero et al., 2014) and boundary conditions (Jacques et al., 2008; Vereecken et al., 2010). Combining high quality soil data with high resolution surface water, GW and meteorological data is an important approach towards a greater understanding of the major controls on P transport to shallow GW and thus provide important knowledge for GW P risk assessments. However, underground storage and release of P to GW and subsequent transit of P to surface water remains poorly understood (Gao et al., 2010).

https://doi.org/10.5194/hess-2020-248
Preprint. Discussion started: 21 July 2020


Hydrology and Earth System Sciences
Discussions

The aim of this study was to address this knowedge gap and was undertaken in a meso-scale catchment observatory in Ireland with pressures assumed to be from GW P pathways. Mellander et al. (2016) had previously showed that long-term dissolved reactive P (DRP) concentrations at the stream outlet were consistently above the Environmental Quality Standard (EQS) of 0.035 mg P L^{-1}. Initial testing of a multi-level borehole network in a connected hillslope revealed spatial and temporal fluctuations in P concentrations. Therefore, the present study examined the connected hillslope in greater detail with three objectives to:

1) determine soil hydraulic properties controlling hydrological P transport to GW along the hillslope;
2) examine variations in GW P concentrations in relation to dynamic physical controls;
3) reveal contrasting physical controls on P transport to GW at the hillslope scale.

2. Materials and methods

2.1. Site description

The meso-scale agricultural catchment (7.58 km^2) (Fealy et al., 2010) is located in the south-west of Ireland (Co. Cork). A summary of catchment characteristics and long-term outlet concentrations of total dissolved P (TDP), DRP, dissolved unreactive P (DUP = TDP – DRP), iron (Fe) and dissolved organic carbon (DOC) are presented in **Table 1**. The catchment is dominated by well drained soils (based on diagnostic features of the soil profile to 1 m and a soil survey at 1:25 000) and permeable bedrock, which results in high levels of infiltration and a GW fed main river (Dupas et al., 2017a; Mellander et al., 2016).

https://doi.org/10.5194/hess-2020-248
Preprint. Discussion started: 21 July 2020

Hydrology and Earth System Sciences
Discussions

107 Table 1: Summary of dominant catchment characteristics.

Average annual rainfall[a]	1 125 mm
Average effective rainfall[a]	600 mm
Soil type	Typical Brown Earth and Typical Brown Podzols (84 %)
Dominant Soil Drainage class	Well drained
Geology	Highly permeable sandstone, mudstone and siltstone
Land use	Grassland (84 %), Arable (6 %)
Outlet water chemistry[b]	0.119 mg TDP L^{-1}, 0.078 mg DRP L^{-1}, 0.029 mg DUP L^{-1}, 0.41 mg Fe L^{-1}, 1.08 mg DOC L^{-1}

108 [a]Meteorological station located within the catchment see Figure 1, 2010-2016

109 [b]Monthly grab samples taken within the catchment see Figure 1, 2010-2016 (DOC 2012-2016)

110

111 The hillslope study site consists of a transect of multi-level piezometers installed to monitor
112 GW level, gradients and water quality (**Fig. 1**). For the purpose of the present study only the
113 shallow piezometers were used at the downslope (DS), midslope (MS) and upslope (US)
114 locations (**Fig. 1, Fig. 2**). Piezometer screen depths were 4-7 m at DS, 10.5-13.5 m at MS and
115 13-16 m at US. Monthly grab samples were taken for chemical analysis using a 200 ml double
116 valve bailer (Solinst, Canada). Samples were filtered (0.45 µm Sartorius) and TDP and DRP
117 were analysed by spectrophotometry after alkaline persulphate oxidation (Askew, 2005) and
118 after ascorbic acid reduction (MDL: 0.005 mg L^{-1}) (Askew and Smith, 2005), respectively.
119 Iron and manganese (Mn) were analysed on a Varian Vista-MPX CCD-Simultaneous ICP-
120 OES (Gottler and Piwoni, 2005), DOC was analysed by a non-Diffractive Infra-Red (NDIR)
121 detector after acidification and combustion (Baird, 2005) and nitrate ($N\text{-}NO_3^-$) was calculated
122 as the difference between total oxidized nitrogen (TON) and nitrite ($N\text{-}NO_2^-$) analysed on a
123 Aquakem 600A (Thermo Scientific, Finland) after hydrazine reduction (MDL: 0.1 mg L^{-1})

https://doi.org/10.5194/hess-2020-248
Preprint. Discussion started: 21 July 2020

Hydrology and Earth System Sciences
Discussions
Open Access
EGU

and phosphoric acid diazotization (MDL: 0.006 mg L^{-1}), respectively (Kamphake et al., 1967). At time of sampling in the field the oxidation reduction potential (ORP) was measured using an Aquaread AP-700 multiparameter probe. Water level and gradients between multi-level piezometers was recorded at high resolution using a Solinst water level logger to ascertain direction of recharge – infiltration *versus* up-welling. Average (2010-2016) depths to GW level (DGWL) were 0.30 ± 0.01 m at DS, 7.20 ± 0.28 m at MS and 11.9 ± 0.23 m at US.

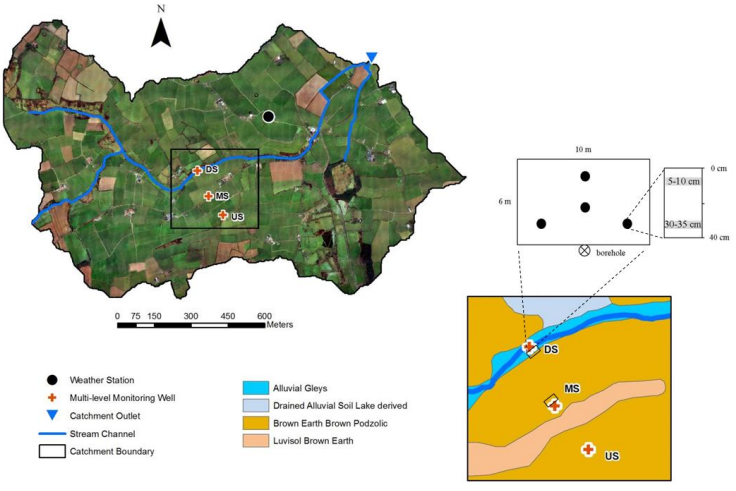

Figure 1 (in color) : Location of the hillslope piezometers (DS, MS and US) within the context of the catchment, stream channel and outlet. The schematic on the lower right indicates soil types and intact coring location and depth of sampling around DS and MS.

https://doi.org/10.5194/hess-2020-248
Preprint. Discussion started: 21 July 2020

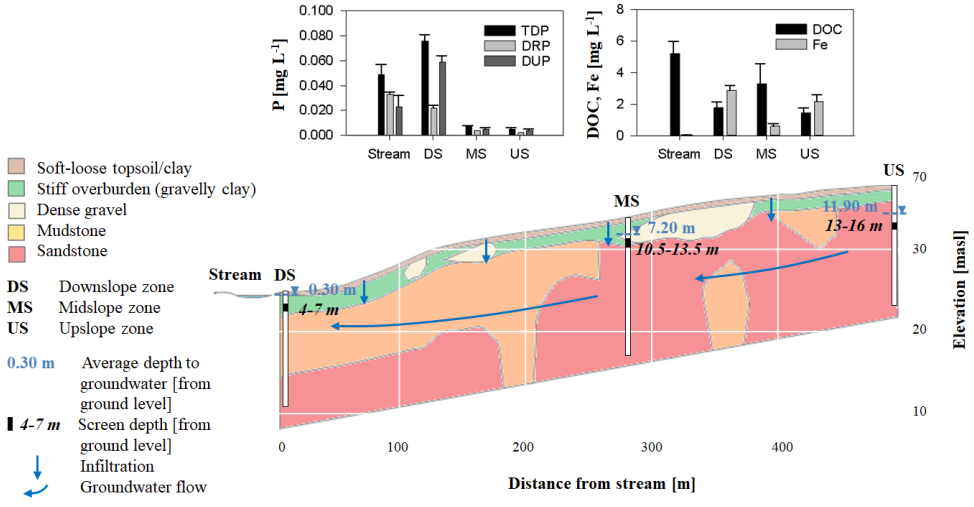

Figure 2 (in color): Geological cross section of the study hillslope showing the location of the piezometers (McAleer et al., 2017; Mellander et al., 2014). Also illustrated are the stream and the groundwater chemistry at the study sites (based on monthly grab samples, 2010-2016 - DOC 2013-2016).

Using long terms datasets average concentrations of dissolved P and related parameters are shown in **Figure 2**. Site DS had higher P concentrations than at MS and in terms of DRP the stream data indicated long-term (2010-2016) average concentrations above or close to the EQS. It should be noted that there are soil type (based on 1 m depth only) differences at DS and MS/US with Humic Alluvial Gley/Gleyic Brown Alluvial soil Typical Brown Earth/Podzols, respectively.

2.2. Field methods - meteorological and soil data

For the purposes of the present study meteorological data taken from a Campbell Scientific BWS-200 weather station (**Fig. 1**) from January 2017 to December 2017 were examined. Absence of rainfall for at least 12 hours was used to separate one rainfall event from another

https://doi.org/10.5194/hess-2020-248
Preprint. Discussion started: 21 July 2020


Hydrology and Earth System Sciences
Discussions

(Ibrahim et al., 2013; Kurz et al., 2005) and only events having at least 5 mm rainfall were included in this process. These data were further sub-divided into 5 rainfall event types (A-E) depending on the total rainfall amount (A = 5.0-9.9 mm, B = 10.0-19.9 mm, C = 20.0-29.9 mm, D = 30.0-39.9 mm, E = ≥40 mm). Using the hybrid soil moisture deficit (SMD) model of Schulte et al. (2005) infiltration [mm] was estimated. Both rainfall and SMD data were used during the interpretation of GW TDP concentrations data and to develop modelling scenarios to explain differences in P concentrations over time at DS and MS locations.

Undisturbed soil cores (8 cm diameter, 5 cm height) were extracted at two depths (5 to 10 cm, 30 to 35 cm, 4 replicates) within a sampling grid close to DS and MS (**Fig. 1**). Using this strategy, 16 soil cores were collected between January and March 2018 before organic fertiliser (i.e. cattle slurry) was applied.

2.3. Laboratory methods

2.3.1. Undisturbed soil physical and hydraulic data

Soil texture was determined using disturbed soil samples taken at both locations and depths which were used to ascertain particle size distribution (PSD, sand, silt and clay content [%] (Brady and Weil, 2008)) using the pipette method (Avery and Bascomb, 1974). Soil ρ_b [g cm^{-3}] was measured using the disturbed soil samples and subsequently using the destructed undisturbed soil cores following soil physics hydraulic analysis. This was preferred to the direct determination via soil water retention curve (SWRC) analysis as results were distorted by the presence of stones in the undisturbed soil cores. Samples were oven-dried at 105 °C for 48 h and then weighed. Stones were extracted, weighed and their volume was determined. The ρ_b was calculated by dividing the soil dry weight by the soil volume.

https://doi.org/10.5194/hess-2020-248
Preprint. Discussion started: 21 July 2020


Hydrology and Earth System Sciences
Discussions

The undisturbed cores were transferred to the laboratory for the continuous hydraulic measurement of a SWRC in terms of volumetric water content θ_v using an evaporation method. The Hyprop apparatus (UMS GmbH, Munich, Germany) (Bezerra-Coelho et al., 2018) was used for this purpose and a detailed procedure has been described in Bacher et al. (2019). In summary, the raw Hyprop data from the direct SWRC approach were then fitted to the bimodal van Genuchten model of Durner (Durner, 1994) with the Mualem-constraint (Mualem, 1976) to obtain the hydraulic parameters needed for the modelling phase. This model is a weighted superposition of two van Genuchten functions and is more suitable than the unimodal models to describe the retention functions of structured soils. It also fitted better to the data than the unimodal constrained model of van Genuchten (1980). The detailed SWRC modelling steps and procedures are described in **S1** in the Supplement.

Hydraulic retention and conductivity parameters were then generated for each soil core: soil residual θ_r and saturated θ_s water contents [cm^3 cm^{-3}], soil K_s [cm d^{-1}], SWRC shape parameters n_1 and n_2 [undimentional; -], α_1 and α_2 [cm^{-1}] and ω_2 [-]. A statistical analysis (E_{RMS}) quantified the quality of the fits for both retention and conductivity.

To further interpret varied conditions at DS and MS additional parameters that could control transport to GW were calculated including total porosity ϕ [%], air capacity ε [%], macro-, meso- and microporosity [%]. Detailed calculation steps are presented in **S2**.

2.3.2. Modelling scenarios of phosphorus hydrological transport to groundwater

Simulations were conducted using Hydrus 1D (Šimůnek et al., 2008; Šimůnek et al., 2013), coupled with appropriate meteorological and soil physical data, boundary conditions, and

https://doi.org/10.5194/hess-2020-248
Preprint. Discussion started: 21 July 2020

Hydrology and Earth System Sciences
Discussions

resulting breakthrough curves were used to assess P hydrological transport to GW at DS and MS (**Fig. 3**).

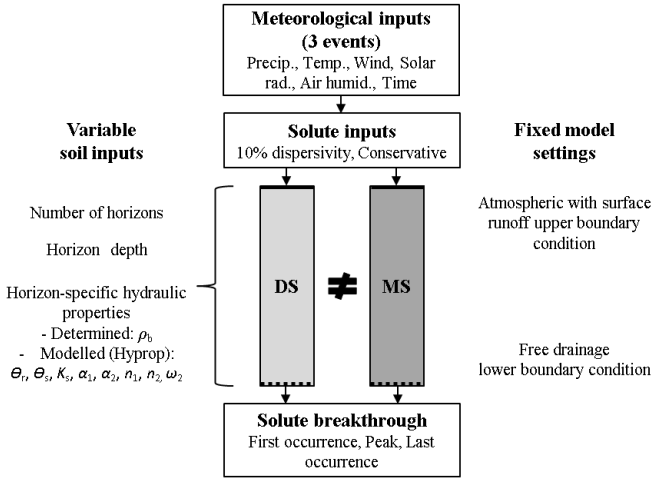

Figure 3: Conceptual diagram indicating input parameters, boundary conditions, soil horizon characteristics and model outputs.

Examination of soil profiles at both sites resulted in the delineation of soil horizons and the determination of the soil profile depths (55 cm for both sites). To build a soil profile for the model the physical and hydraulic data taken from the undisturbed cores were used for both DS and MS locations. Specifically θ_r and θ_s [$cm^3\ cm^{-3}$], K_s [$cm\ h^{-1}$], SWRC shape parameters α_1 and α_2 [cm^{-1}], n_1 and n_2 [-], ω_2 [-] and soil ρ_b [$g\ cm^{-3}$] were used as input parameters. For each depth the replicate which showed the best fit (E_{RMS}) to the retention and conductivity models was chosen. Hydraulic data of the selected soil core were applied to the soil horizon including this soil core sampling depth and when no hydraulic data were available for a horizon, the data from the upper horizon were applied. For each location DS and MS, one model run was carried out for each rainfall event (R1, R2 and R3) leading to six model scenarios in total.

https://doi.org/10.5194/hess-2020-248
Preprint. Discussion started: 21 July 2020


Hydrology and Earth System Sciences
Discussions

Atmospheric upper boundary conditions with surface runoff were assigned to the model. Hourly (Vero et al., 2014) total precipitation (cm), maximum and minimum temperatures [ºC], average wind speed [km d^{-1}], average solar radiation [MJ cm^{-2}] and average air humidity [%] data from 2017 were used as input parameters. Solute dispersivity was set at 10 % of soil profile depth (Fetter, 2008; Šimůnek et al., 2013). A conservative solute was used in order to examine the role of soil hydraulic properties on the potential for P transport to GW. Thus, no soil chemical input data were used in the models and chemical P attenuation processes in soil are not considered here. Conservative solute initial concentration at the soil surface was set at 10 mmol cm^{-1} and 1 cm precipitation was applied with no evaporation, in order to initiate vertical solute movement into the soil profile. Free drainage was specified as the lower boundary condition (Jacques et al., 2008).

2.4. Data and statistical analysis

For objective 1, analysis of variance (ANOVAs) was used to investigate significant ($P < 0.05$) difference of soil properties between depths within each site and between sites for each depth. Residuals plots were used to assess the normal distribution of the residuals and the equal variance of the data; data were log transformed before statistical analyses when those conditions were not met. Trends were studied when the variation between replicates was very high (e.g. K_s). Pearson r correlations were used to measure the degree of relationship between soil parameters. Statistical analysis was carried out using R Studio 3.5.2.

3. Results

3.1. Soil hydraulic properties

https://doi.org/10.5194/hess-2020-248
Preprint. Discussion started: 21 July 2020


Hydrology and Earth System Sciences
Discussions

Detailed soil physical and hydraulic data for all undisturbed soil cores replicates of sites DS and MS are shown in Table **S3** and Table **S4**, respectively. Below is a description of the overall (at the scale of the sampling area, including the four replicates) variations observed between sites and depths. The SWRC shape parameters α_1 and α_2, n_1 and n_2, ω_2, as well as θ_s and θ_r are not presented as they are not considered to be the main parameters controlling hydrological transport to GW. A detailed description of hydraulic parameters is presented in **S5**. Soil at DS is a Sandy Loam whereas MS soil has a Loamy texture.

Average soil ρ_b was higher (not significantly) at MS than DS for both shallow and deeper soil cores. Average soil ρ_b increased with depth (not significantly) in each site: from 0.89 ± 0.05 g cm^{-3} to 0.95 ± 0.03 g cm^{-3} at DS, and from 1.20 ± 0.05 g cm^{-3} to 1.27 ± 0.05 g cm^{-3} at MS. Soil organic matter (OM %) was higher at DS (8.3 %) than at MS (4.6 %).

At both sites and for both depths, soil K_s were variable. Average K_s was higher (not significantly) at MS than DS for both shallow and deeper soil cores. Average K_s decreased with depth (not significantly) at each site: from 1 648 ± 791 to 829 ± 600 cm d^{-1} at DS, and from 2 981 ± 1 417 to 2 242 ± 1 248 cm d^{-1} at MS.

Average ϕ was higher (not significantly) at DS than MS for both shallow and deeper soil cores. Average ϕ decreased with depth (not significantly) at each site: from 66 ± 2 % to 64 ± 1 % at DS, and from 54 ± 2 % to 51 ± 2 % at MS. Average ε was higher (not significantly) at DS than MS for both shallow and deeper soil cores. Average ε increased with depth (not significantly) at each site: from 22 ± 5 % to 24 ± 2 % at DS, and from 14 ± 1 % to 19 ± 2 % at MS.

https://doi.org/10.5194/hess-2020-248
Preprint. Discussion started: 21 July 2020


Hydrology and Earth System Sciences
Discussions
Open Access
EGU

Average soil macroporosity was higher (not significantly) at DS than MS for both shallow and deeper soil cores. Average soil macroporosity significantly decreased with depth at MS; from 45 ± 2 % to 35 ± 4 % but not significantly at DS; from 49 ± 2 % to 40 ± 5 %. Average soil mesoporosity was the same at DS and MS for both shallow and deeper soil cores and decreased with depth (not significantly) from 6 ± 3 % to 4 ± 2 %. Average soil microporosity was the same at DS and MS for both shallow and deeper soil cores and decreased (not significantly) with depth from 2 ± 1 to 1 ± 1 %.

Soil ρ_b was strongly and significantly correlated to sand (r = - 0.828), silt (r = 0.792) and clay % (r = 0.833) as was soil ϕ (r = 0.828, r = - 0.794, r = - 0.829, respectively). Air capacity was correlated to clay % (r = - 0.503).

Soil physical and hydraulic data used as input parameters in Hydrus 1D are presented in **Table 2**, only the replicate showing the best fit (E_{RMS}) to the retention and conductivity models was chosen. Values were in accordance with the overall tendencies observed between/within depths and sites and explained previously. An exception exists for the K_s values due to the variability between replicates.

https://doi.org/10.5194/hess-2020-248
Preprint. Discussion started: 21 July 2020

Hydrology and Earth System Sciences
Discussions

Table 2: Summary of soil physical and hydraulic data used as input parameters in Hydrus 1D.

Site	Horizon depth	θ_r	θ_s	α_1	n_1	K_s	l	ω_2	α_2	n_2	ρ_b
		$cm^3\ cm^{-3}$	$cm^3\ cm^{-3}$	cm^{-1}	-	$cm\ h^{-1}$	-	-	cm^{-1}	-	$g\ cm^{-3}$
DS	0-23 cm	0.00	0.63	0.500	1.816	80	0.5	0.618	0.004	1.256	0.84
	23-43 cm	0.00	0.51	0.177	2.159	120	0.5	0.737	0.090	1.135	0.86
	43-55 cm	0.00	0.51	0.177	2.159	120	0.5	0.737	0.090	1.135	0.86
MS	0-25 cm	0.00	0.51	0.001	1.449	18	0.5	0.483	0.191	1.198	1.30
	25-55 cm	0.00	0.44	0.306	1.311	43	0.5	0.410	0.001	1.629	1.40

3.2. Rainfall events, soil moisture deficit, water table depth and groundwater quality

Rainfall during 2017 is presented in **Figure 4a**. During this year 56 rainfall events were categorised as follows: 18 events A, 21 events B, 6 events C, 9 events D and 2 events E (Table **S6**, A = 5.0-9.9 mm, B = 10.0-19.9 mm, C = 20.0-29.9 mm, D = 30.0-39.9 mm, E = ≥40 mm).

https://doi.org/10.5194/hess-2020-248
Preprint. Discussion started: 21 July 2020

Hydrology and Earth System Sciences
Discussions

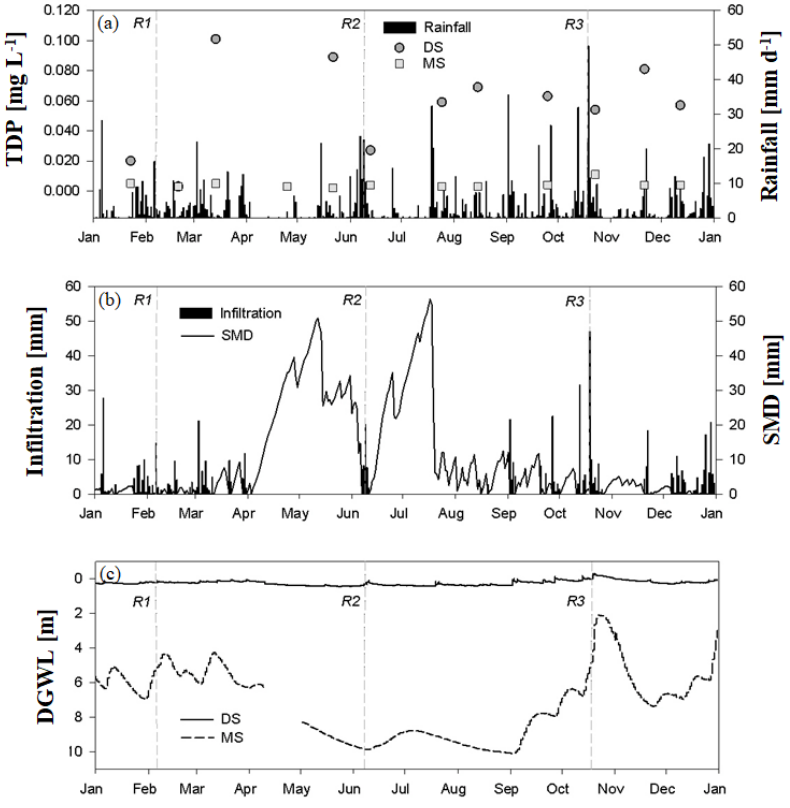

Figure 4: Evolution of (a) monthly groundwater TDP concentrations at sites DS (circle) and MS (square) and daily rainfall, (b) daily infiltration and soil moisture deficit and (c) depth to GWL over the study year 2017. Locations of the three study rainfall events (R1, R2 and R3) are also shown.

Rainfall event R1 [B; long duration with low total rainfall] occurred from the 6th to 7th of February, R2 [D; short duration with high total rainfall] from the 9th to 10th of June and R3 [E; long duration with high total rainfall] from the 18th to 19th of October. Event and pre-event characteristics are shown in **Figure 5**. Total rainfall was the highest for R3 and the smallest for R1 (50.6 and 19 mm, respectively), while maximum rainfall was the smallest for R1 (3.2 mm h^{-1}) and comparable between R2 and R3 (6.2 and 6.4 mm h^{-1}, respectively). Rainfall

https://doi.org/10.5194/hess-2020-248
Preprint. Discussion started: 21 July 2020

Hydrology and Earth System Sciences
Discussions

308 event R3 was the longest (40 h) while R2 was the shortest (15 h). Infiltration during the event
309 was the highest for R3 and the lowest for R1 (47.1 and 16.8 mm, respectively). Pre-event total
310 rainfall (previous 7 days) was the lowest for R1 (25.4 mm) and was comparable between R2
311 and R3 (55.8 and 57.2 mm, respectively).
312

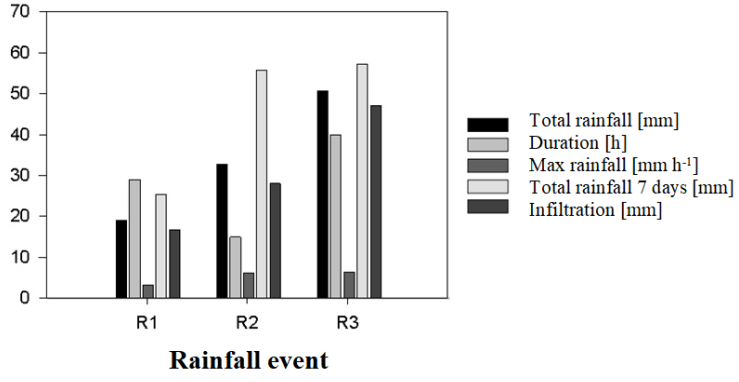

313
314 Figure 5: Summary of events and pre-events characteristics.
315

316 Daily SMD and infiltration for sites DS and MS (well drained) over the year 2017 are shown
317 in **Figure 4b**. Frequent rainfall from January to March and from September to December led
318 to SMD less than 10 mm and frequent infiltration with a peak of 47 mm occurring in mid-
319 October. From April to July, less rainfall led to increasing SMD with two peaks in mid-May
320 and mid-July above 50 mm. However, rainfall in late May - early June decreased SMD and
321 led to infiltration in early June. Rainfall of July-August also decreased SMD but did not lead
322 to ED, occurring later in September. In total, 95 days of infitration occurred during the year
323 2017, mainly between January and March (42 days), September and December (46 days) but
324 also very briefly in June (5 days) and August (2 days). Depth to GWL (DGWL) for both sites
325 is shown in **Figure 4c**. At MS, DGWL was between 2 and 10 m with variations through the
326 year. Depth to GWL increased in April (to reach 8-10 m) due to low rainfall and high SMD

https://doi.org/10.5194/hess-2020-248
Preprint. Discussion started: 21 July 2020


Hydrology and Earth System Sciences
Discussions

and remained high until September-October. At this time of the year and until December, DGWL was lower due to low SMD and high rainfall leading to infiltration and GW recharge. At DS, DGWL was lower than at MS (up to 40 cm in April-September) with GWL sometimes above the ground level (September-December).

Over the year 2017, concentrations in TDP were higher at DS than at MS with a higher variability in concentrations at DS (**Fig. 4a**). In particular, TDP concentrations at DS were comparable to concentrations at MS on some occasions (January, February, April, June) whereas they were contrasted on other occasions (March, May, July-December).

3.3. Modelled hydrological transport to groundwater

Modelled tracer breakthrough curves at the bottom of the DS and MS soil profiles are shown in **Figure 6** for each rainfall event R1 [B; long duration with low total rainfall] (**Fig. 6a**), R2 [D; short duration with high total rainfall] (**Fig. 6b**) and R3 [E; long duration with high total rainfall] (**Fig. 6c**). Tracer first and last occurrences, concentration peak and total transport duration are shown in **Table 3**.

https://doi.org/10.5194/hess-2020-248
Preprint. Discussion started: 21 July 2020

Hydrology and Earth System Sciences
Discussions

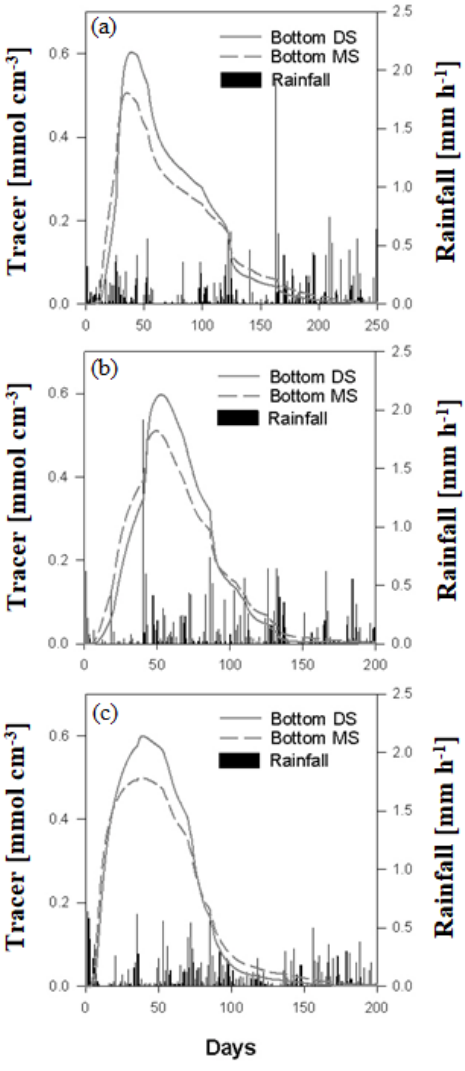

Figure 6: Tracer breakthrough curves at the bottom of the soil profiles DS and MS for rainfall events (a) R1 [B; long duration with low total rainfall], (b) R2 [D; short duration with high total rainfall] and (c) R3 [E; long duration with high total rainfall]

https://doi.org/10.5194/hess-2020-248
Preprint. Discussion started: 21 July 2020

Table 3: Tracer breakthrough characteristics at sites DS and MS for rainfall events R1, R2 and R3.

Site	Rainfall event	First occurrence (days)	Peak (days)	Last occurrence (days)	Total transport duration (days)
DS	R1	12	42	212	200
	R2	9	50	150	141
	R3	5	37	158	153
MS	R1	8	35	237	229
	R2	6	46	193	186
	R3	4	36	183	180

Tracer first occurrence occurred later at DS than at MS for all rainfall events whereas the last occurrence always occurred earlier at DS than at MS. More precisely, tracer first occurrence at DS occurred 12 days, 9 days and 5 days after tracer injection and 8 days, 6 days and 4 days after tracer injection at MS during rainfall events R1, R2 and R3, respectively. Tracer last occurrence at DS occurred 212 days, 150 days and 158 days after injection and 237 days, 193 days and 183 days after tracer injection at MS during rainfall events R1, R2 and R3, respectively. Hence, the total tracer transport duration was lower at DS than at MS for all rainfall events. Tracer concentration peak occurred earlier at MS than at DS for all rainfall events. At MS, it occurred 35 days, 46 days and 36 days after tracer injection, during rainfall events R1, R2 and R3, respectively. At DS, it occurred 42 days, 50 days and 37 days after tracer injection, during rainfall events R1, R2 and R3, respectively. Tracer concentration peak was also higher at DS (0.60 mmol cm^{-3}) than at MS (0.50 mmol cm^{-3}) for all rainfall events.

https://doi.org/10.5194/hess-2020-248
Preprint. Discussion started: 21 July 2020


Hydrology and Earth System Sciences
Discussions

364

365 Tracer first occurrence occurred earlier during R3 [E; long duration with high total rainfall]
366 for both sites DS and MS. Tracer last occurrence also occurred earlier during R3 but only at
367 site MS, it occurred earlier during R2 [D; short duration with high total rainfall] at site DS.
368 Total tracer transport duration was higher during R1 [B; long duration with low total rainfall]
369 for both sites whereas it was lower during R2 at DS and during R3 at MS. Tracer
370 concentration peak occurred earlier during R3 at both sites but also during R1 at MS. It
371 occurred later during R2 at both sites.

372

373 **4. Discussion**

374 This study highlighted the spatial variability of P hydrological transport through the soil
375 profile to GW within a hillslope of contrasting GW P concentrations, and examined the inter-
376 annual variability of GW P concentrations. A range of modelled hydraulic properties and
377 transport capacities were identified to 1) determine static soil hydraulic properties controlling
378 hydrological transport to GW along the hillslope, 2) examine variations in GW P
379 concentrations in relation to dynamic physical controls and 3) reveal contrasting physical
380 controls on the potential for P transport to GW at the hillslope scale. The combined analysis
381 of meteorological data, high resolution soil physical/hydraulic data and GW chemical data
382 revealed contrasting spatial and temporal P hydrological transport potential to GW along the
383 hillslope in relation to the existence of a static system (soil) and a dynamic system (rainfall,
384 GWL, soil moisture), respectively. The DS zone showed a higher hydrological transport
385 potential with favourable soil properties and geochemical processes towards high and
386 variable GW P concentrations. The MS zone was characterised by limited hydrological
387 transport potential.

388

https://doi.org/10.5194/hess-2020-248
Preprint. Discussion started: 21 July 2020


Hydrology and Earth System Sciences
Discussions

389 **4.1. Spatial variability in hydrological transport to groundwater**

390 The potential for hydrological transport to GW varies within the same hillslope and is
391 determined by soil physical and hydraulic properties. The undisturbed soil cores study
392 suggested that there was a higher potential for hydrological P transport to GW in the DS zone
393 (**Fig. 7**) due to a lower soil compaction (bulk density ρ_b) and higher soil K_s. This was
394 supported by the Hydrus 1D scenario modelling, where flashier tracer transport and higher
395 concentration peaks were evident (**Table 3**, **Fig. 6**), and which was independent of the type of
396 rainfall event (duration, total rainfall). In contrast, the MS zone was more compacted (higher
397 soil ρ_b) with lower soil K_s, suggesting an attenuation of hydrological P transport to GW (**Fig.**
398 **7**). This was supported by the modelling indicating longer total tracer transport duration with
399 lower concentration peaks, independent of the type of rainfall event, even though the tracer
400 first occurrence appeared earlier in the MS zone (**Table 3, Fig. 6**). Higher ϕ, ε and
401 macroporosity measured from undisturbed soil cores were also characteristics of the DS zone
402 supporting the higher potential for hydrological P transport in this zone. High temporal
403 resolution monitoring of GWL (**Fig. 4c**) also revealed a quick recharge of the aquifer at DS
404 (although GWL is higher at this location) after rainfall events with a slow recovery to original
405 water table position whereas at MS reaction to rainfall was slower.
406
407

https://doi.org/10.5194/hess-2020-248
Preprint. Discussion started: 21 July 2020

Hydrology and Earth System Sciences
Discussions
Open Access
EGU

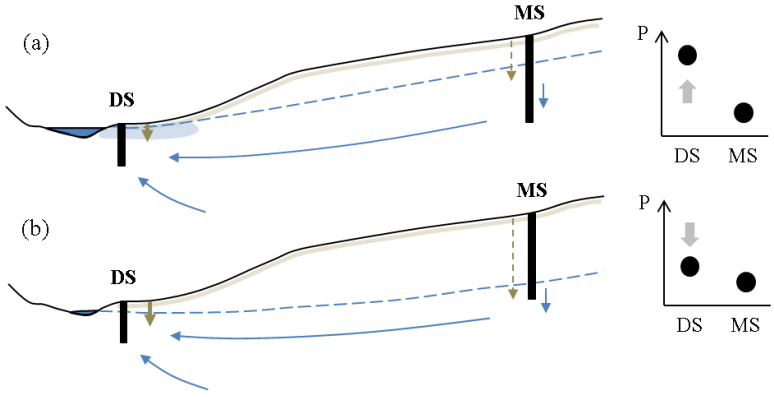

Figure 7 (in color): Schematic of contrasting groundwater P concentrations scenarios: (a) contrasting concentrations between the DS and MS zones with higher P concentrations in the DS zone due to the hydrological connection with soil P and (b) similar concentrations between the DS and MS zones with lower P concentrations in the DS zone due to the hydrological disconnection with soil P. In both scenarios the DS zone evidence a higher potential for P hydrological transport to groundwater: shorter transport duration through the soil profile and transport distance to groundwater.

Observed spatial variability of soil hydraulic properties is supported by DeFauw et al. (2014) who evaluated hydraulic properties of surface soils at varying micro-topographic positions and found that the infiltration rates were approximately twofold higher at the micro-topographic low position (thicker soil) than at the high position (thinner soil). However, other studies found that saturated hydraulic properties at the position with a thinner soil were higher than at the position with a thicker soil (Dai et al., 2019). In this study, there was no significant difference in soil thickness at DS and MS (**Table 2**). However, there was a difference in soil texture. The differences in percentage of sand, silt and clay may explain the variability in soil hydraulic properties, since hydraulic conductivities are coupled to the grain size distribution of soils (Mahmoodlu et al., 2016; Pachepsky and Rawls, 2003; Pachepsky et

https://doi.org/10.5194/hess-2020-248
Preprint. Discussion started: 21 July 2020


Hydrology and Earth System Sciences
Discussions

al., 2006). In this study, soil ρ_b and ϕ were linked to percentage of sand, silt and clay and indicated that sandy soils have more potential for hydrological transport to GW whereas clay soils can attenuate transport as soil ε was negatively correlated to the percentage clay. Even if soil ρ_b increased with depth at both sites and may thus attenuate hydrological transport along the soil profile, the shallower GWL at DS may reach the upper soil layers exhibiting higher hydrological transport potential and lead to shorter P transport distances (**Fig. 7**).

However, the present study focused only on the topsoil (first 40 cm) and further work is needed to have a more complete understanding of the vertical physical variability/heterogeneity of the deeper soil, especially where the GW table is deeper as it is the case at the MS location. Soil chemical properties have also to be considered, especially in soils rich in P-binding materials (Fe, Al, Ca, clay, OM), to take into account possible attenuation processes (sorption/desorption, precipation/dissolution) occurring along the soil profiles and controlling P transport to GW (timing, concentration). For this transect in particular, the DS zone showed evidence of higher soil OM %, labile inorganic P and degree of P saturation (DPS) (measured in composite soil samples – not presented here) that could enhance the amount of P transported to GW whereas the MS zone evidence higher soil total Fe possibly attenuating P transport.

4.2. Inter-annual variability in hydrological transport to groundwater

The potential for hydrological transport to GW also varied within the same hillslope zone and appeared to be linked to the inter-annual dynamic of other physical controls (GWL, soil moisture, rainfall), as observed over the year 2017. Seasonal variations in GW P concentrations revealed at the DS zone by monthly monitoring appeared to be, in part, controlled by GWL fluctuations. Shallower GW, especially after rainfall events or during wet

https://doi.org/10.5194/hess-2020-248
Preprint. Discussion started: 21 July 2020


Hydrology and Earth System Sciences
Discussions

periods (August – December) (**Fig. 7a**), may led to reductive dissolution of soil Fe hydroxides being solubilised as Fe^{2+} and releasing P previously adsorbed (Vidon et al., 2010), a mechanism observed under anoxic conditions (Carlyle and Hill, 2001). This can be important in this zone where chemical tests on composite soil samples revealed a higher DPS than at the MS zone (not presented here). Previous monitoring of the GW also showed low $N\text{-}NO_3^-$ concentration (mean annual concentrations of 0.03 ± 0.01 mg L^{-1}) due to denitrifying conditions (mean annual ORP of 6.0 ± 1.8 mV) (McAleer et al., 2017) and higher Fe (4 712 ± 1 526 µg L^{-1}) and Mn (2 928 ± 197 mg L^{-1}) concentrations compared to the MS zone; this supports the hypothesis of Fe oxyhydroxide reduction. Dupas et al. (2015) showed that soil solution P concentrations in riparian wetlands were strongly linked to GWL dynamics. Shallow GWL may connect with and mobilise more soil P as the pool and/or mobility of soil P decreases with depth, this is especially important as a higher soil labile inorganic P content has been measured at DS compared to MS. Organic riparian soils are known as internal sources of soluble reactive P (Dupas et al., 2017b; Gu et al., 2017; Records et al., 2016) due to poor retention capacities (Daly et al., 2001; Roberts et al., 2017) and their high proportion in a catchment has been strongly related to higher stream soluble reactive P concentrations (Dupas et al., 2018). At the MS zone, the soil showed lower soil labile inorganic P, DPS and higher total Fe contents than at DS possibly attenuating P in GW, also deeper at this location. Moreover, hydrochemical GW data revealed nitrification processes (mean annual ORP of 162.5 ± 3.5 mV) occurring (McAleer et al., 2017). This site had higher annual mean $N\text{-}NO_3^-$ concentration (7.21 ± 0.38 mg L^{-1}) but lower Fe (3.85 ± 0.87 µg L^{-1}) and Mn concentrations (2.87 ± 0.74 mg L^{-1}) than at the DS zone. This suggests that reduction of Fe hydroxides is limited and may support low GW P concentrations measured at this site. However, as the GW table sinks during dry periods in the DS zone in April, or later in the year in the MS zone (**Fig. 7b**), it may leave the higher P sources in the topsoil disconnected.

https://doi.org/10.5194/hess-2020-248
Preprint. Discussion started: 21 July 2020


Hydrology and Earth System Sciences
Discussions

Soil moisture conditions also appeared to be important as soil rewetting after dry periods could explain peaks in GW P concentrations in May (**Fig. 4a, 4b**), revealed by monthly GW monitoring, through release of microbial P by osmotic shock (Blackwell et al., 2010; Turner and Haygarth, 2001) or loss of colloidal P (1-1000 nm) *via* preferential flowpaths in macropores (Poulsen et al., 2006; Vendelboe et al., 2011). Morover, monthly monitoring of GW also revealed contrasting P concentrations between February (DS lower and comparable to MS) and October (DS higher, MS lower) where soil moisture conditions were comparable (**Fig. 4a, 4b**). This could be related to rainfall patterns as the Hydrus 1D scenario modelling showed that tracer first occurrence and peak appeared earlier during rainfall event R3 [October; long duration with high total rainfall] than during rainfall event R1 [February; long duration with low total rainfall]. Tracer total transport duration was also lower during rainfall event R3 than R1 (**Table 3**) suggesting that P reaction time with the soil matrix is lower and attenuation processes are more limited during this type of rainfall event, thus potentially explaining higher GW P concentrations.

However, P concentrations measured in GW can result from a combination of vertical P leaching from soil and lateral flows within the aquifer transporting P from the upper hillslope which are not considered here. Further work is needed including acquisition of higher resolution GW chemical data to get a better understanding of the main processes explaining inter-annual P dynamics, especially in the near stream zone DS. Inclusion of the different P species and fractions, including colloidal P, would be an important improvement into understanding such processes. Monitoring of stream P fractions and species and determination of hydrological pathways would also be important to determine the contribution of the different hillslope zones. Indeed, previous research in catchments with

https://doi.org/10.5194/hess-2020-248
Preprint. Discussion started: 21 July 2020


Hydrology and Earth System Sciences
Discussions

similar shallow GW systems and presence of riparian wetlands have shown that seasonal variability of stream soluble reactive P was linked to the contribution of different hillslope compartments (Dupas et al., 2017a).

.

4.3. Physical controls on phosphorus hydrological transport to groundwater

Higher monthly GW P concentrations were observed in the DS zone where the undisturbed soil cores study revealed favourable soil hydraulic properties (lower soil compaction, higher K_s, Sandy Loam soil, higher macroporosity) towards higher hydrological transport potential (**Fig. 7**), independantly of the type of rainfall event as supported by the Hydrus 1D modelling scenarios. Contrasting GW P concentrations were also measured in the DS zone over the year and may be due to Fe hydroxides reduction triggered by the fluctuations of the GW table connected with higher P source in this zone (**Fig. 7a**). On the opposite, the MS zone had more potential to attenuate GW P concentrations with higher soil compaction, lower K_s, Loamy soil and deeper GW table (**Fig. 7**). Hence, it appeared that mitigation strategies to reduce GW P concentrations at the hillslope scale should focus on the DS zone even though deeper GW flowpaths from the MS zone or upslope could be a potential source of P to the DS zone as multi-level piezometric GW monitoring evidenced upwelling of deeper GW in this zone.

Remediation measures should prioritise reducing the source of soil P by limiting the timing and/or the intensity of the grazing period especially during periods of higher GW table that may mobilise P. Reduction of P applications (as synthetic or organic fertilizers) on the MS zone and the upslope should also be considered due to time lags (Vero et al., 2017) of P transport to the DS zone and attenuation processes occurring along the transfer pathways. However, the long-term legacy of P in soil (Jarvie et al., 2013) might lead to a slow depletion of P accumulated in soils. Moreover, interactions between P and NO_3^- have to be carefully

https://doi.org/10.5194/hess-2020-248
Preprint. Discussion started: 21 July 2020


Hydrology and Earth System Sciences
Discussions

527 considered and further strategies to reduce NO_3^- in the nitrification zone MS could result in
528 increasing GW P concentrations, even though it has been suggested that P release by
529 reductive dissolution of Fe hydroxides only needs low NO_3^- concentrations to take place
530 (Dupas et al., 2018).
531
532 **5. Conclusion**
533 Both static and dynamic factors influence hillslope P transport to shallow GW and therefore P
534 concentrations can vary both spatially and temporally over short distances. Herein, two
535 conceptual views of the hillslope emerged. The first corresponds to similar and low
536 concentrations between the DS and MS zones due to less connection between GW and soil P
537 and also longer P travel time within the soil profile where P attenuation processes can occur,
538 even though the DS zone has more potential for hydrological transport due to its physical and
539 hydraulic properties. The second corresponds to contrasting concentrations between the DS
540 and MS zones with the DS zone becoming temporally elevated due to the hydrological
541 connection (high GWL) with soil P and shorter travel time within the soil profile. Hence, soil
542 physical and hydraulic properties are important for hydrological transport to GW and should
543 be considered to better target cost-effective mitigation measures by prioritising reduction of P
544 sources (grazing limitation, reduction of P applications on the connected hillslope) in zones
545 of high potential for hydrological transport as the DS zone. Here they are characterised by a
546 lower soil compaction, higher K_s and a sandy soil texture.
547
548 **Author contribution**
549 MF: Conceptualization, Methodology, Validation, Formal analysis, Investigation, Data
550 curation, Writing – original draft, Writing – reviewing and editing, Visualization. OF:
551 Conceptualization, Methodology, Validation, Resources, Writing – reviewing and editing,

https://doi.org/10.5194/hess-2020-248
Preprint. Discussion started: 21 July 2020

552 Supervision. PEM: Conceptualization, Methodology, Resources, Writing – reviewing and
553 editing, Funding acquisition. PJ and KD: Conceptualization, Methodology, Writing –
554 reviewing and editing.
555
556 **Competing interests**
557 The authors declare that they have no conflict of interest.
558
559 **Acknowledgements**
560 We thank the land owners and farmers of the fields for cooperation and sampling permission,
561 the ACP staff especially David Ryan and Dermot Leahy for field sampling assistance, Una
562 Cullen for meteorological and GW level data supply. The lab work of Shane Scannell for
563 bulk density analyses is greatly appreciated. We also thank Matthias Bacher for Hyprop
564 training and Cathal Somers for help in Hyprop lab set up and particle size analyses. Funding
565 was provided by the Department of Agriculture, Food and the Marine through the
566 Agricultural Catchments Programme and by the Teagasc Walsh Fellowship Programme.
567
568 **References**
569 Anderson, A. E., Weiler, M., Alila, Y., and Hudson, R. O.: Dye staining and excavation of
570 a lateral preferential flow network, Hydrol. Earth Syst. Sci., 13, 935–944, 2009.
571 Askew, F. E.: Persulfate method for simultaneous determination of total nitrogen and total
572 phosphorus. 4500-P J, in: Eaton, A. D., Clesceri, L. S., Rice, W. E., and Greenberg, A. E.,
573 editors. Standard Methods for the Examination of Water and Wastewater, 21st edition. ISBN
574 0-87553-047-8. 800 1 street, NW Washington, DC 2001-3710: American Public Health
575 Association, 160-161, 2005.

https://doi.org/10.5194/hess-2020-248
Preprint. Discussion started: 21 July 2020

576 Askew, F. E. and Smith, R. K.: Inorganic non metallic constituents; Phosphorus; Method
577 4500-P F. Automated ascorbic acid reduction method, in: Eaton, D. A., Clesceri, L. S.,
578 Rice, E. W., and Greensberg, A. E., editors. Standard Methods for the Examination of
579 Waters and Waste Water. 800 1 street, NW Washington, DC 2001-3710: ISBN 0-87553-
580 047-8 American Public Health Association, 4-155, 2005.
581 Avery, B. W. and Bascomb, C. L.: Soil survey laboratory methods.: Soil Survey of Great
582 Britain (England and Wales), Harpenden (Rothamsted Experimental Station, Harpenden,
583 Herts.), 1974.
584 Bacher, M. G., Schmidt, O., Bondi, G., Creamer, R., and Fenton, O.: Comparison of Soil
585 Physical Quality Indicators Using Direct and Indirect Data Inputs Derived from a
586 Combination of In-Situ and Ex-Situ Methods, Soil Science Society of America Journal,
587 83, 5-17, 2019.
588 Bachmair, S. and Weiler, M.: Hillslope characteristics as controls of subsurface flow
589 variability, Hydrol. Earth Syst. Sci., 16, 3699–3715, 2012a.
590 Bachmair, S., Weiler, M., and Troch, P. A.: Intercomparing hillslope hydrological dynamics:
591 spatio–temporal variability and vegetation cover effects, Water Resour. Res., 48, 2012b.
592 Baird, R. B.: Aggregate organic constituents; Total Organic Carbon (TOC)/Method 5310 B
593 High temperature combustion methods, in: Eaton, D. A., Clesceri, L. S., Rice, E. W., and
594 Greensberg, A. E., editors. Standard Methods for the Examination of Waters and Waste
595 Water. 21st ed. ISBN 0-87553-047-8. 800 1 street, NW Washington, DC 2001-3710:
596 American Public Health Association, 5-21, 2005.
597 Bezerra-Coelho, C. R., Zhuang, L., Barbosa, M. C., Soto, M., and van Genuchten, M. T.:
598 Further tests of the HYPROP evaporation method for estimating the unsaturated soil
599 hydraulic properties, Journal of Hydrology and Hydromechanics, 66(2), 161-169, 2018.

https://doi.org/10.5194/hess-2020-248
Preprint. Discussion started: 21 July 2020

600 Blackwell, M. S. A., Brookes, P. C., de la Fuente-Martinez, N., Gordon, H., Murray, P. J.,
601 Snars, K. E. et al. Chapter 1 - Phosphorus Solubilization and Potential Transfer to Surface
602 Waters from the Soil Microbial Biomass Following Drying–Rewetting and Freezing–
603 Thawing. Advances in Agronomy, 106, 1-35, 2010.
604 Bol, R., Julich, D., Brödlin, D., Siemens, J., Kaiser, K., Dippold, M. A. et al.: Dissolved and
605 colloidal phosphorus fluxes in forest ecosystems—an almost blind spot in ecosystem
606 research, J Plant Nutr Soil Sci., 179, 425-438, 2016.
607 Brady, N.C. and Weil, R. R.: The Nature and Properties of Soils, 14th Edition. United States
608 of America: Pearson Education Inc., 2008.
609 Bünemann, E. K., Bongiorno, G., Bai, Z., Creamer, R. E., De Deyn, G., de Goede, R. et al.:
610 Soil quality – A critical review, Soil Biology and Biochemistry, 120, 105-125, 2018.
611 Carlyle, G. C. and Hill, A. R.: Groundwater phosphate dynamics in a river riparian zone:
612 effects of hydrologic flowpaths, lithology and redox chemistry, Journal of Hydrology, 247,
613 151-168, 2001.
614 Cordell, D. and White, S.: Life's Bottleneck: Sustaining the World's Phosphorus for a Food
615 Secure Future, Annual Review of Environment and Resources, 39, 161, 2014.
616 Dai, C., Wang, T., Zhou, Y., Deng, J., and Li, Z.: Hydraulic Properties in Different Soil
617 Architectures of a Small Agricultural Watershed: Implications for Runoff Generation,
618 Water, 11(12), 2537, 2019.
619 Daly, K., Jeffrey, D., and Tunney, H.: The effect of soil type on phosphorus sorption capacity
620 and desorption dynamics in Irish grassland soils, Soil Use Manage., 17, 12-20, 2001.
621 DeFauw, S. L., Brye, K. R., Sauer, T. J., and Hays, P.: Hydraulic and Physiochemical
622 Properties of a Hillslope Soil Assemblage in the Ozark Highlands, Soil Sci., 179(3), 107-
623 117, 2014.

https://doi.org/10.5194/hess-2020-248
Preprint. Discussion started: 21 July 2020

624 Duan, J., Yang, J., Tang, C., Chen, L., Liu, Y., and Wang, L.: Effects of rainfall patterns and
625 land cover on the subsurface flow generation of sloping Ferralsols in southern China,
626 PLOS ONE, 12(8), 2017.
627 Dupas, R., Gruau, G., Gu, S., Humbert, G., Jaffrézic, A., and Gascuel-Odoux, C.:
628 Groundwater control of biogeochemical processes causing phosphorus release from
629 riparian wetlands, Water Research, 84, 307-314, 2015.
630 Dupas, R., Mellander, P-E., Gascuel-Odoux, C., Fovet, O., McAleer, E. B., McDonald, N. T.
631 et al.: The role of mobilisation and delivery processes on contrasting dissolved nitrogen
632 and phosphorus exports in groundwater fed catchments, Science of The Total
633 Environment, 599-600, 1275-1287, 2017a.
634 Dupas, R., Musolff, A., Jawitz, J. W., Rao, P. S. C., Jäger, C. G., Fleckenstein, J. H. et al.:
635 Carbon and nutrient export regimes from headwater catchments to downstream reaches,
636 Biogeosciences, 14, 4391–4407, 2017b.
637 Dupas, R., Tittel, J., Jordan, P., Musolff, A., and Rode, M.: Non-domestic phosphorus release
638 in rivers during low-flow: Mechanisms and implications for sources identification, Journal
639 of Hydrology, 560, 141-149, 2018.
640 Durner, W.: Hydraulic conductivity estimation for soils with heterogeneous pore structure,
641 Water Resour Res., 30, 211-223, 1994.
642 Fealy, R. M., Buckley, C., Mechan, S., Melland, A., Mellander, P-E., Shortle, G. et al.: The
643 Irish Agricultural Catchments Programme: catchment selection using spatial multi-criteria
644 decision analysis, Soil Use Manage., 26, 225-236, 2010.
645 Fenton, O., Vero, S., Ibrahim, T. G., Murphy, P. N. C., Sherriff, S. C., and Ó hUallacháin, D.:
646 Consequences of using different soil texture determination methodologies for soil physical
647 quality and unsaturated zone time lag estimates, Journal of Contaminant Hydrology, 182,
648 16-24, 2015.

https://doi.org/10.5194/hess-2020-248
Preprint. Discussion started: 21 July 2020


Hydrology and Earth System Sciences
Discussions

649 Fenton, O., Mellander, P-E., Daly, K., Wall, D. P., Jahangir, M. M. R., Jordan, P. et al.:
650 Integrated assessment of agricultural nutrient pressures and legacies in karst landscapes,
651 Agriculture, Ecosystems & Environment, 239, 246-256, 2017.
652 Fetter, C.: Contaminant Hydrogeology, 2nd Edition Long Grove: Waveland Press Inc., 2008.
653 Fuchs, J. W., Fox, G. A., Storm, D. E., Penn, C. J., and Brown, G. O.: Subsurface Transport
654 of Phosphorus in Riparian Floodplains: Influence of Preferential Flow Paths, Journal of
655 Environmental Quality, 38(2), 473-484, 2009.
656 Gao, Y., Zhu, B., Wang, T., Tang, J. L., Zhou, P., and Miao, C. Y.: Bioavailable phosphorus
657 transport from a hillslope cropland of purple soil under natural and simulated rainfall,
658 Environmental Monitoring and Assessment, 171, 539-550, 2010.
659 Gladnyeva, R. and Saifadeen, A. Effects of hysteresis and temporal variability in
660 meteorological input data in modelling of solute transport in unsaturated soil using
661 Hydrus-1D, Journal Of Water Resources Planning And Management, 68, 285-293, 2013.
662 Gottler, R. A., and Piwoni, M. D.: Metals.
663 Method 3120 B. Inductively coupled plasma (ICP) method, in: Eaton, D. A., Clesceri, L.
664 S., Rice, E. W., and Greensberg, A. E., editors. Standard Methods for the Examination of
665 Waters and Waste Water. 21st ed. 800 1 street, NW Washington, DC 2001-3710:
666 American Public Health Association, 3-39, 2005.
667 Graham, C. B., Woods, R. A., and McDonnell, J. J.: Hillslope threshold response to rainfall:
668 (1) A field based forensic approach, J. Hydrol., 393, 65–76, 2010.
669 Gu, S., Gruau, G., Dupas, R., Rumpel, C., Crème, A., Fovet, O. et al.: Release of dissolved
670 phosphorus from riparian wetlands: Evidence for complex interactions among
671 hydroclimate variability, topography and soil properties, Science of The Total
672 Environment, 598, 421-431, 2017.

https://doi.org/10.5194/hess-2020-248
Preprint. Discussion started: 21 July 2020

673 Guo, L., Lin, H., Fan, B., Nyquist, J., Toran, L., and Mount, G. J.: Preferential flow through
674 shallow fractured bedrock and a 3D fill-and-spill model of hillslope subsurface hydrology,
675 Journal of Hydrology, 576, 430-442, 2019.
676 Ibrahim, T. G., Fenton, O., Richards, K. G., Fealy, R. M., and Healy, M. G.: Spatial and
677 temporal variations of nutrient loads in overland flow and subsurface drainage from a
678 marginal land site in south-east Ireland, Biology and Environment: Proceedings of the
679 Royal Irish Academy, 113B(2), 1-18, 2013.
680 Jacques, D., Šimůnek, J., Mallants, D., and van Genuchten, M. T.: Modelling coupled water
681 flow, solute transport and geochemical reactions affecting heavy metal migration in a
682 podzol soil, Geoderma, 145, 449-461, 2008.
683 Jarvie, H. P., Sharpley, A. N., Spears, B., Buda, A. R., May, L., and Kleinman, P. J.: Water
684 Quality Remediation Faces Unprecedented Challenges from "Legacy Phosphorus",
685 Environ Sci Technol., 47(16), 8997-8998, 2013.
686 Julich, D., Julich, S., and Feger, K.: Phosphorus fractions in preferential flow pathways and
687 soil matrix in hillslope soils in the Thuringian Forest (Central Germany), J Plant Nutr Soil
688 Sci., 180, 407-417, 2017.
689 Kamphake, L. J., Hannah, S. A., and Cohen, J. M.: Automated analysis for nitrate by
690 hydrazine reduction, Water Res., 1, 205-216, 1967.
691 Kurz, I., Coxon, C., Tunney, H., and Ryan, D.: Effects of grassland management practices
692 and environmental conditions on nutrient concentrations in overland flow, Journal of
693 Hydrology, 304, 35-50, 2005.
694 Lehmann, P., Hinz, C., McGrath, G., Tromp-van-Meerveld, H. J., and McDonnell, J. J.:
695 Rainfall threshold for hillslope outflow: an emergent property of flow pathway
696 connectivity, Hydrol. Earth Syst. Sci., 11, 1047-1063, 2007.

https://doi.org/10.5194/hess-2020-248
Preprint. Discussion started: 21 July 2020

697 Lintern, A., Webb, J. A., Ryu, D., Liu, S., Bende-Michl, U., Waters, D. et al.: Key factors
698 influencing differences in stream water quality across space. WIREs Water, 5: e1260,
699 2018.
700 Mabilde, L., De Neve, S., and Sleutel, S.: Regional analysis of groundwater phosphate
701 concentrations under acidic sandy soils: Edaphic factors and water table strongly mediate
702 the soil P-groundwater P relation, Journal of Environmental Management, 203(1), 429-
703 438, 2017.
704 Mahmoodlu, M. G., Raoof, A., Sweijen, T., and van Genuchten, M. T.: Effects of Sand
705 Compaction and Mixing on Pore Structure and the Unsaturated Soil Hydraulic Properties,
706 Vadose Zone Journal, 15(8), 2016.
707 McAleer, E. B., Coxon, C. E., Richards, K. G., Jahangir, M. M. R., Grant, J., and Mellander,
708 P-E.: Groundwater nitrate reduction versus dissolved gas production: A tale of two
709 catchments, Science of The Total Environment, 586, 372-389, 2017.
710 McGinley, P. M., Masarik, K. C., Gotkowitz, M. B., and Mechenich, D. J.: Impact of
711 anthropogenic geochemical change and aquifer geology on groundwater phosphorus
712 concentrations, Applied Geochemistry, 72, 1-9, 2016.
713 Melland, A. R., Mellander, P-E., Murphy, P. N. C., Wall, D. P., Mechan, S., Shine, O. et al.:
714 Stream water quality in intensive cereal cropping catchments with regulated nutrient
715 management, Environmental Science & Policy, 24, 58-70, 2012.
716 Mellander, P-E., Melland, A. R., Murphy, P. N. C., Wall, D. P., Shortle, G., and Jordan, P.:
717 Coupling of surface water and groundwater nitrate-N dynamics in two permeable
718 agricultural catchments, The Journal of Agricultural Science, 152, 107-124, 2014.
719 Mellander, P-E., Jordan, P., Shore, M., McDonald, N. T., Wall, D. P., Shortle, G. et al.:
720 Identifying contrasting influences and surface water signals for specific groundwater
721 phosphorus vulnerability, Science of The Total Environment, 541, 292-302, 2016.

https://doi.org/10.5194/hess-2020-248
Preprint. Discussion started: 21 July 2020

722 Mellander, P-E., Jordan, P., Bechmann, M., Fovet, O., Shore, M., McDonald, N. T. et al.
723 Integrated climate-chemical indicators of diffuse pollution from land to water, Scientific
724 Reports, 8, 944, 2018.
725 Mualem, Y.: A new model for predicting the hydraulic conductivity of unsaturated porous
726 media, Water Resour Res., 12, 513-522, 1976.
727 Neidhard, H., Schoeckle, D., Schleinitz, A., Eiche, E., Berner, Z., Tram, P. T. K. et al.:
728 Biogeochemical phosphorus cycling in groundwater ecosystems – Insights from South and
729 Southeast Asian floodplain and delta aquifers, Science of the Total Environment, 644,
730 1357-1370, 2018.
731 Pachepsky, Y. A. and Rawls, W. J.: Soil structure and pedotransfer functions, Eur J Soil Sci.,
732 54, 443-452, 2003.
733 Pachepsky, Y. A., Rawls, W. J., and Lin, H. S.: Hydropedology and pedotransfer functions,
734 Geoderma, 131, 308-316, 2006.
735 Pang, L., Lafogler, M., Knorr, B., McGill, E., Saunders, D., Baumann, T. et al.: Influence of
736 colloids on the attenuation and transport of phosphorus in alluvial gravel aquifer and
737 vadose zone media, Science of The Total Environment, 550, 60-68, 2016.
738 Poulsen, T. G., Moldrup, P., de Jonge, L. W., and Komatsu, T.: Colloid and Bromide
739 Transport in Undisturbed Soil Columns, Vadose Zone Journal, 5, 649-656, 2006.
740 Records, R. M., Wohl, E., and Arabi M.: Phosphorus in the river corridor, Earth-Science
741 Reviews, 158, 65-88, 2016.
742 Roberts, W. M., Gonzalez-Jimenez, J. L., Doody, D. G., Jordan, P., and Daly, K.: Assessing
743 the risk of phosphorus transfer to high ecological status rivers: Integration of nutrient
744 management with soil geochemical and hydrological conditions, Science of The Total
745 Environment, 589, 25-35, 2017.

https://doi.org/10.5194/hess-2020-248
Preprint. Discussion started: 21 July 2020

746 Schilling, K. E., Kim, S., Jones, C. S., and Wolter, C. F.: Orthophosphorus Contributions to
747 Total Phosphorus Concentrations and Loads in Iowa Agricultural Watersheds, Journal of
748 Environmental Quality, 46(4), 828-835, 2017.
749 Schoumans, O. F. and Groenendijk, P.: Modeling Soil Phosphorus Levels and Phosphorus
750 Leaching From Agricultural Land In the Netherlands, Journal of environmental quality,
751 29(1), 111-116, 2000.
752 Schoumans, O. F., Silgram, M., Groenendijk, P., Bouraoui, F., Andersen, H. E., Kronvang,
753 B. et al. Description of nine nutrient loss models: capabilities and suitability based on their
754 characteristics, Journal of Environmental Monitoring, 11(3), 5066-5114, 2009.
755 Schulte, R. P. O., Diamond, J., Finkele, K., Holden, N. M., and Brereton, A. J.: Predicting the
756 soil moisture conditions of Irish grassland, Irish Journal of Agriculture and Food
757 Research, 44(1), 95-110, 2005.
758 Sharpley, A. N.: Managing agricultural phosphorus to minimize water quality impacts,
759 Scientia Agricola, 73(1), 1-8, 2016.
760 Šimůnek, J., van Genuchten, M. T., and Sejna, M.: Modeling subsurface water flow and
761 solute transport with HYDRUS and related numerical software packages. In: Navarro PG,
762 Playán E, editors. Numerical Modelling of Hydrodynamics for Water Resources., 2008.
763 Šimůnek, J., Šejna, M., Saito, H., Sakai, M, and van Genuchten, M. T.: The HYDRUS 1D
764 software package for simulating the movement of water, heat and
765 multiple solutes in variably saturated media. Version 4.16 HYDRUS software series
766 Riverside, California, USA.: Department of Environmental Science, University of
767 California Riverside, 2013.
768 Sinha, E., Michalak, A. M., and Balaji, V.: Eutrophication will increase during the 21st
769 century as a result of precipitation changes, Science, 357, 407-408, 2017.

https://doi.org/10.5194/hess-2020-248
Preprint. Discussion started: 21 July 2020

770 Tromp-van Meerveld, H. J. and Weiler, M.: Hillslope dynamics modeled with increasing
771 complexity, J. Hydrol., 361, 24–40, 2008.
772 Turner, B. and Haygarth, P.: Biogeochemistry - Phosphorus solubilization in rewetted soils,
773 Nature, 411, 258, 2001.
774 Vendelboe, A. L., Moldrup, P., Heckrath, G., Jin, Y., and de Jonge, L. W.: Colloid and
775 Phosphorus Leaching From Undisturbed Soil Cores Sampled Along a Natural Clay
776 Gradient, Soil Sci., 176(8), 399-406, 2011.
777 Vereecken, H., Javaux, M., Weynants, M., Pachepsky, Y., Schaap, M., and van Genuchten,
778 M. T.: Using pedotransfer functions to estimate the van genuchten- mualem soil hydraulic
779 properties: A review, Vadose Zone Journal, 9(4), 795-820, 2010.
780 Vero, S. E., Ibrahim, T. G., Creamer, R. E., Grant, J., Healy, M. G., Henry, T. et al.:
781 Consequences of varied soil hydraulic and meteorological complexity on unsaturated zone
782 time lag estimates, Journal of Contaminant Hydrology, 170, 53-67, 2014.
783 Vero, S. E., Healy, M. G., Henry, T., Creamer, R. E., Ibrahim, T. G., Richards, K. G. et al.: A
784 framework for determining unsaturated zone water quality time lags at catchment scale,
785 Agriculture, Ecosystems & Environment, 236, 234-242, 2017.
786 Vidon, P., Allan, C., Burns, D., Duval, T. P., Gurwick, N., Inamdar, S. et al.: Hot Spots and
787 Hot Moments in Riparian Zones: Potential for Improved Water Quality Management,
788 Journal of the American Water Resources Association, 46, 278-298, 2010.
789 Withers, P. J. A., Neal, C., Jarvie, H. P., and Doody, D. G.: Agriculture and Eutrophication:
790 Where Do We Go from Here?, Sustainability, 6, 5853-5875, 2014.